1.55-μm mode-locked quantum-dot lasers with 300 MHz frequency tuning range

Cite as: Appl. Phys. Lett. **106**, 031114 (2015); https://doi.org/10.1063/1.4906451
Submitted: 06 November 2014 . Accepted: 12 January 2015 . Published Online: 22 January 2015

T. Sadeev, D. Arsenijević, D. Franke, J. Kreissl, H. Künzel, and D. Bimberg

1.55-μm mode-locked quantum-dot lasers with 300 MHz frequency tuning range

T. Sadeev,[1,a)] D. Arsenijević,[1] D. Franke,[2] J. Kreissl,[2] H. Künzel,[2] and D. Bimberg[1,b)]
[1]*Institut für Festkörperphysik, Technische Universität Berlin, 10623 Berlin, Germany*
[2]*Heinrich-Hertz-Institut, Einsteinufer 37, 10587 Berlin, Germany*

(Received 6 November 2014; accepted 12 January 2015; published online 22 January 2015)

Passive mode-locking of two-section quantum-dot mode-locked lasers grown by metalorganic vapor phase epitaxy on InP is reported. 1250-μm long lasers exhibit a wide tuning range of 300 MHz around the fundamental mode-locking frequency of 33.48 GHz. The frequency tuning is achieved by varying the reverse bias of the saturable absorber from 0 to −2.2 V and the gain section current from 90 to 280 mA. 3 dB optical spectra width of 6–7 nm leads to ex-facet optical pulses with full-width half-maximum down to 3.7 ps. Single-section quantum-dot mode-locked lasers show 0.8 ps broad optical pulses after external fiber-based compression. Injection current tuning from 70 to 300 mA leads to 30 MHz frequency tuning. © *2015 AIP Publishing LLC*.
[http://dx.doi.org/10.1063/1.4906451]

Passively mode-locked semiconductor lasers (MLLs) are able to emit as low as fs-short optical pulses at frequencies up to tens of GHz without any external frequency source.[1] MLLs are of largest importance, e.g., for ultra-high data rate optical transmission, signal processing, clock sources, and biomedicine.[1] Significant improvements of the performance of MLL as well as continuous-wave (CW) laser parameters have been achieved in last decades, thanks to implementing zero-dimensional (quantum dot) structures into the active layer.[2,3] Their inherent properties allow to produce lasers with increased temperature stability,[4] low threshold current,[5] fast carrier dynamics,[6] inhomogeneously broadened spectrum, and low amplified spontaneous emission (ASE).[7] Most advantages of QD MLL have been demonstrated for GaAs-based ones, operating at 1310 nm wavelength, targeting short-range telecom applications, where optical fiber exhibits zero dispersion.[8] Long-haul optical transmission systems operate in the 1550 nm range, where fiber losses are minimal. At this wavelength mature and cost effective InP based growth technology is common, but the brake-through results of QD MLLs are much scarcer as compared to their 1310 nm counterparts. Presently reported MOVPE (metal organic vapour phase epitaxy) grown monolithic two-section QD MLLs operate at 10.5 GHz and emit strongly chirped pulses several tens of ps broad.[9] Quantum dashes (QDashes), elongated quantum dots, are believed to have properties close to QDs and have been investigated intensively in several groups. Reports on mode-locking observed in QDash single-section lasers show both ex facet sub picosecond[10] and ps range pulse emission after compression with low timing jitter.[11,12] In Ref. 13 chemical beam epitaxy grown single-section QD laser demonstrates ex facet 295 fs pulses at 50 GHz. The mechanism of pulse generation in such single-section lasers is not well understood. Thus, proper device engineering as a solution to obtain direct ex-facet (i.e., without compression techniques) fs-pulse emission is not yet available, constraining further system implementation of such lasers. QDash two-section lasers, however, demonstrate ex facet ps-pulse emission and repetition frequency up to 20 GHz (Ref. 14) with better control of output pulse train characteristics. The present results obtained for InP based QDash MLLs as well as for GaAs based 1310 nm QD MLLs confirm the advantages of the 3-D carrier confinement approach, but also reveal that QD based full advantages have not been yet realized at 1550 nm.

In this paper, we demonstrate ex-facet ps-range optical pulses at ultra-high repetition rate of InP/InAs based two-section QD MLL. Furthermore, we report on single-section QD MLLs (or SSMLL) made of the same wafer material and located on the same laser bar as two-section QD MLLs. We compare their mode-locking properties and also discuss the mechanism of pulse propagation.

The laser structures are grown by metalorganic vapor phase epitaxy (MOVPE) on n-type (001) InP substrate. The active region consists of 7 stacked QD layers in an $In_{0.78}Ga_{0.22}As_{0.47}P_{0.53}$ matrix. This structure is enclosed by an $In_{0.82}Ga_{0.18}As_{0.40}P_{0.60}$ waveguide. Finally, single-mode laser buried heterostructures are formed by deep etching through the active region and regrowth of p/n-blocking and contact layers. Details of material growth, processing, and results of material characterisation can be found in Ref. 15. Single- and two-section devices are processed from this wafer material. Their length is 1.25 mm and the ridge width is 1 μm in both cases, no coating is applied to the facets. For the two-section devices, the ratio between gain section (GS) and absorber section (AS) is 5.6:1 (≈15% for the absorber). For electrical isolation of the GS and AS, sections are separated by a 20 μm gap without impacting the optical waveguide properties. Single-section lasers are driven only by electrical pumping of the GS. In the two-section lasers, the sections are operated independently: reverse bias is applied to AS and forward bias to the GS.

Light-current curves measured at room temperature are shown in Fig. 1(a) both for single- and two-section lasers. The threshold current density is 1.57 kA/cm^2, the differential

[a)]Electronic mail: tagir@mailbox.tu-berlin.de
[b)]Also at King Abdulaziz University, 22254 Jeddah, Saudi Arabia.

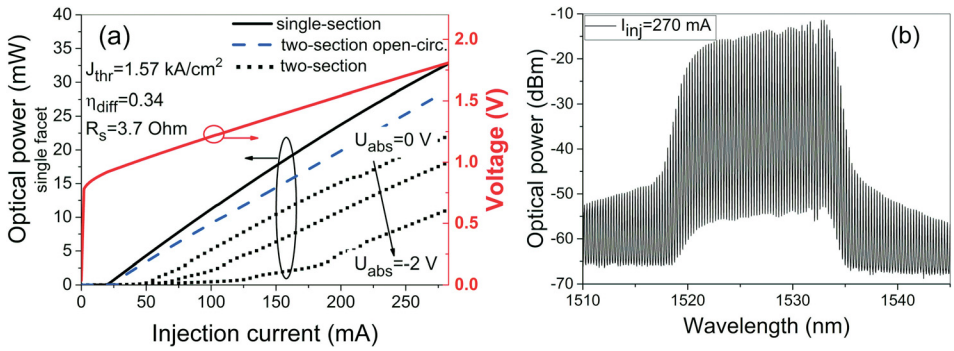

FIG. 1. Light-current characteristics of single-section and two-section devices (a); (b) optical spectrum of a single-section laser at 270 mA.

quantum efficiency is 0.32, maximum output power is 34 mW, the series resistance is 3.7 Ω, and turn-on voltage is equal to 0.78 V for single-section devices. For two-section lasers, an increased threshold current is observed for AS open-circuit and increasing reverse bias due to increasing absorption. An optical spectrum of a single-section device measured at 270 mA ($\approx 13 I_{thr}$) shown in Fig. 1(b), exhibits a peak wavelength at 1533 nm, and a −3 dB 6–7 nm spectral width. The spectrum is broad and uniform due to the inhomogeneous broadening of the QDs.

Passive mode-locking in two-section lasers is first analysed by recording radiofrequency (RF) spectra for each pair of U_{abs}/I_{inj} from −2.2 V to 0 V and from 90 mA to 280 mA, resulting in a RF vs. U_{abs}/I_{inj} map (shown in Fig. 2(a)), considering only pure mode-locking operation, i.e., RF signal-to-noise ratio (SNR) larger than 30 dB in the whole range. The region of mode-locking (ML) is limited by (a) Q-switching (shaded area below left), characterized by the presence of low-frequency oscillations (Fig. 2(a), inset) and their beating products; and (b) CW-lasing, as a result of weak absorption at low U_{abs} (0 V to −0.2 V) and high current ($I_{inj} > 190$ mA). 300 MHz is the tuning range of repetition frequency under ML conditions. The repetition frequency decreases with increasing current I_{inj} at fixed absorber voltage U_{abs}. The thermal expansion of material and reduced refractive index n_{refr} due to carrier escape (caused by temperature induced carrier heating and band gap shrinkage) are the reasons. Second, an increase of reverse U_{abs} at fixed I_{inj} leads to an increase of repetition frequency. We interpret this increase by enhanced absorption leading to a reduced number of photons in the cavity. This in-turn reduces the number of stimulated transitions, meanwhile the exciton population increases due to the pump, thus n_{refr} decreases.[16] The reduction of n_{refr} leads to the increase of repetition frequency.

Single-section lasers also exhibit mode-locking. Their repetition frequency depends on current. The frequency generally increases with current (Fig. 2(b)), corresponding to a reduced n_{refr} due to material dispersion[17] of the waveguide, induced by a red shift of optical spectra by ∼10 nm in the 100–300 mA range. The waveguide thermal expansion (cavity length increases) is the reason for RF decrease at currents beyond 250 mA. The flat region in the middle and the oscillations observed are presently under more detailed investigation. We point out that the repetition frequency of SSMLL is tunable by ∼30 MHz, which is ten times lower than that of the two-section laser mentioned above.

Optical pulse emission of both two- and single-section MLLs is now examined using second-harmonic generation based autocorrelation techniques. For two-section MLL autocorrelation (AC) traces are recorded at operating parameters with stable mode-locking (RF SNR > 30 dB), and without pulse compression (i.e., ex-facet measurement). Pulse FWHM map after deconvolution assuming Gaussian shape pulses is shown in Fig. 3(a). An AC-trace for one particular pair of operating parameters $I_{inj} = 200$ mA, $U_{abs} = -1.0$ V is shown in the inset of Fig. 3(a). We point to the minimum measured pulse FWHM of 3.7 ps. The FWHM increases with increased current at fixed U_{abs}, because at higher current the absorber bleaches faster as pulses carry more power, also gain is enhanced leading to the broadening of the net gain window.[18] On the other hand, at higher $-U_{abs}$ and constant I_{inj}, pulses get shorter due to reduced absorber recovery time as carriers experience a faster escape from the QDs to the barrier.[19,20]

AC measurements are also carried out for SSMLL. Fig. 3(b) shows the measured pulse width after 150 m of standard single-mode fiber used for compression.[21] We observe a Lorentzian shape (pulses in Fig. 3(b), inset) with the lowest pulse FWHM ≈ 0.8 ps (Fig. 3(b)). At low current,

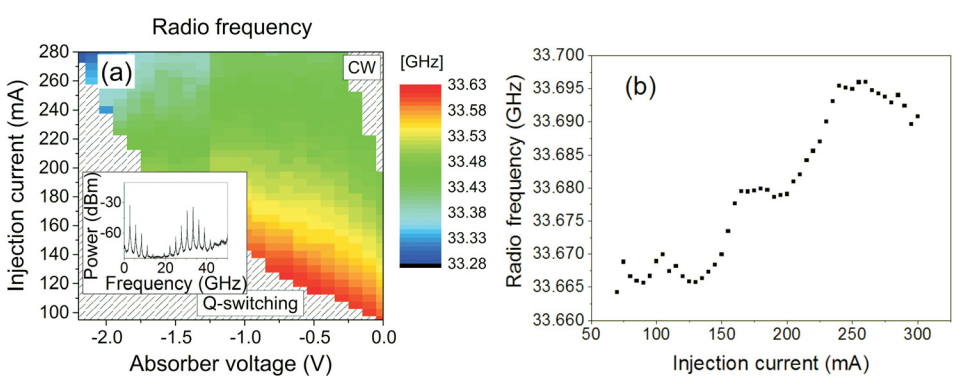

FIG. 2. (a) Repetition frequency colour map of two-section MLL, inset—Q-switched mode-locking regime at $I_{inj} = 220$ mA, $U_{abs} = -1.9$ V. (b) Single-section MLL repetition frequency as a function of injection current.

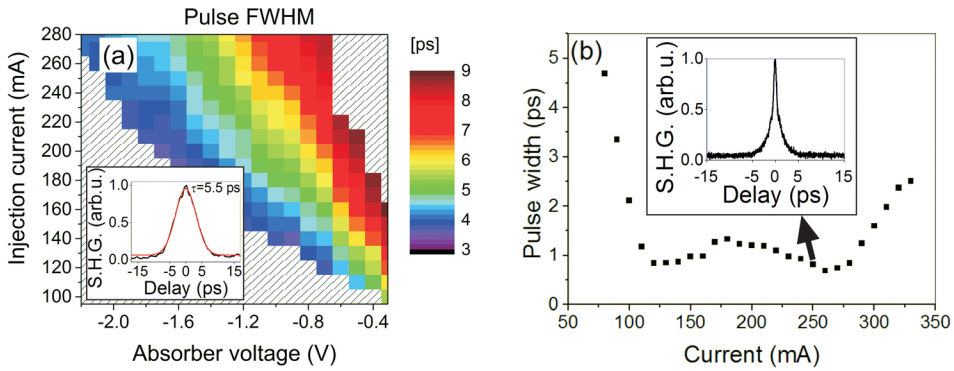

FIG. 3. (a) Pulse width colour map of two-section laser (a), in the inset AC-trace at $I_{inj} = 200$ mA, $U_{abs} = -1.0$ V. (b) Pulse width with AC-trace (inset) after 150 m of single-mode fiber as the functions of current measured for single-section device.

the pulses are broad, because along with lower optical FWHM, the efficiency of $\chi^{(3)}$ is not enough to set up phase correlation between optical modes.[22] With increased current (80–280 mA) more optical modes are excited and intracavity nonlinearities are strong enough to lock their phases, leading to short pulse formation, thus a flat region of the characteristic in Fig. 3(b) is built-up. At currents larger than 280 mA pulse FWHM increases again, which is probably due to the increased number of excited modes inducing unsynchronized phase interference, but, in particular, a larger α-factor and hence increased chirp.[23,24]

We propose the following simplified model for pulse propagation dynamics in SSMLL: during propagation along the cavity two-photon absorption (TPA) creates non-uniform but periodic exciton distributions in the cavity. Since high photon densities within the pulse are reduced via TPA, the photon density is increased by stimulated emission from excitons which are electrically pumped and whose distribution is uniform.[25] Non-uniform distribution of carrier density and third-order nonlinearities are responsible for a complex dependence of refractive index on current, resulting in pulse phase modulation and large chirp which are actually observed in SSMLL.[21]

Timing jitter is characterized through the RF-linewidth[26] and along with high repetition rate, low timing jitter of the pulse train is important for any application. A huge difference between RF-linewidths in two- and single-section MLLs has been observed. For two-section lasers, it is in the order of 2–3 MHz, whereas for single-section MLLs it does not exceed 300 kHz. The reason for the one order of magnitude difference is that the absorber section induces additional losses, thus reducing the ratio between stimulated and spontaneous emission, resulting in an increase of optical phase noise. This in turn broadens the RF-line and increases the timing jitter.[21,26]

To conclude, we demonstrate monolithic two-section true QD MLLs at 1.55 μm with better performance than yet reported. The lasers exhibit a wide range of operating parameters with stable mode locking. 300 MHz of the repetition frequency tuning for RF SNR > 30 dB is observed. Autocorrelation shows ex-facet Gaussian shape optical pulse emission. Lowest optical pulse FWHM is 3.7 ps without any compression at 33.5 GHz repetition rate. We also investigated the ML properties of single-section lasers made of the same wafer material. The repetition frequency of single-section mode-locked laser is found to be less tuneable, ~30 MHz around 33.68 GHz. The FWHM measured after fibre compression demonstrates two local minima at 130–150 mA and 260–270 mA of approximately 0.8 ps. We discussed the variation of the pulse FWHM and repetition frequency under varying operating parameters in both types of devices. The control of pulse width and repetition frequency is more efficient in two-section lasers.

This work has been supported by Collaborative Research Centre 787 (SFB 787) of German Research Foundation (Deutsche Forschungsgemeinschaft-DFG) and Seventh Framework Programme through PROPHET Initial Training Network.

[1]D. Bimberg, J. Phys. D: Appl. Phys. **38**, 2055 (2005).
[2]D. Bimberg, Electron. Lett. **44**, 168 (2008).
[3]C. Gilfert, V. Ivanov, N. Oehl, M. Yacob, and J. P. Reithmaier, Appl. Phys. Lett. **98**, 201102 (2011).
[4]O. B. Shchekin and D. G. Deppe, Appl. Phys. Lett. **80**, 3277 (2002).
[5]R. L. Sellin, C. Ribbat, M. Grundmann, N. N. Ledentsov, and D. Bimberg, Appl. Phys. Lett. **78**, 1207 (2001).
[6]O. Karni, K. J. Kuchar, A. Capua, V. Mikhelashvili, G. Sęk, J. Misiewicz, V. Ivanov, J. P. Reithmaier, and G. Eisenstein, Appl. Phys. Lett. **104**, 121104 (2014).
[7]J. Gomis-Bresco, S. Dommers-Völkel, O. Schöps, Y. Kaptan, O. Dyatlova, D. Bimberg, and U. Woggon, Appl. Phys. Lett. **97**, 251106 (2010).
[8]M. Kuntz, G. Fiol, M. Lämmlin, D. Bimberg, M. G. Thompson, K. T. Tan, C. Marinelli, R. V. Penty, I. H. White, V. M. Ustinov, A. E. Zhukov, Y. M. Shernyakov, and A. R. Kovsh, Appl. Phys. Lett. **85**, 843 (2004).
[9]M. J. R. Heck, A. Renault, E. A. J. M. Bente, Y.-S. Oei, M. K. Smit, K. S. E. Eikema, W. Ubachs, S. Anantathanasarn, and R. Notzel, IEEE J. Sel. Top. Quantum Electron. **15**, 634 (2009).
[10]G.-H. Duan, A. Shen, A. Akrout, F. Van Dijk, F. Lelarge, F. Pommereau, O. LeGouezigou, J.-G. Provost, H. Gariah, F. Blache, F. Mallecot, K. Merghem, A. Martinez, and A. Ramdane, Bell Labs Tech. J. **14**, 63 (2009).
[11]K. Klaime, C. Calò, R. Piron, C. Paranthoen, D. Thiam, T. Batte, O. Dehaese, J. Le Pouliquen, S. Loualiche, A. Le Corre, K. Merghem, A. Martinez, and A. Ramdane, Opt. Express **21**, 29000 (2013).
[12]K. Merghem, C. Calo, R. Rosales, X. Lafosse, G. Aubin, A. Martinez, F. Lelarge, and A. Ramdane, IEEE J. Quantum Electron. **50**, 275 (2014).
[13]Z. G. Lu, J. R. Liu, P. J. Poole, Z. J. Jiao, P. J. Barrios, D. Poitras, J. Caballero, and X. P. Zhang, Opt. Commun. **284**, 2323 (2011).
[14]E. Sooudi, G. Huyet, J. G. McInerney, F. Lelarge, K. Merghem, R. Rosales, A. Martinez, A. Ramdane, and S. P. Hegarty, IEEE Photonics Technol. Lett. **23**, 1544 (2011).
[15]D. Franke, J. Kreissl, W. Rehbein, F. Wenning, H. Kuenzel, U. W. Pohl, and D. Bimberg, Appl. Phys. Express **4**, 014101 (2011).
[16]B. R. Bennett, R. A. Soref, and J. del Alamo, IEEE J. Quantum Electron. **26**, 113 (1990).
[17]P. Runge, R. Elschner, and K. Petermann, IEEE J. Quantum Electron. **46**, 644 (2010).
[18]H. Haus, IEEE J. Sel. Top. Quantum Electron. **6**, 1173 (2000).
[19]E. A. Viktorov, T. Erneux, P. Mandel, T. Piwonski, G. Madden, J. Pulka, G. Huyet, and J. Houlihan, Appl. Phys. Lett. **94**, 263502 (2009).

[20]D. B. Malins, A. Gomez-Iglesias, S. J. White, W. Sibbett, A. Miller, and E. U. Rafailov, Appl. Phys. Lett. **89**, 171111 (2006).
[21]R. Rosales, K. Merghem, A. Martinez, A. Akrout, J.-P. Tourrenc, A. Accard, F. Lelarge, and A. Ramdane, IEEE J. Sel. Top. Quantum Electron. **17**, 1292 (2011).
[22]R. Rosales, S. G. Murdoch, R. T. Watts, K. Merghem, A. Martinez, F. Lelarge, A. Accard, L. P. Barry, and A. Ramdane, Opt. Express **20**, 8649 (2012).
[23]M. Osinski and J. Buus, IEEE J. Quantum Electron. **23**, 9 (1987).
[24]S. Schneider, P. Borri, W. Langbein, U. Woggon, R. L. Sellin, D. Ouyang, and D. Bimberg, IEEE J. Quantum Electron. **40**, 1423 (2004).
[25]H. Ju, A. V. Uskov, R. Nötzel, Z. Li, J. M. Vázquez, D. Lenstra, G. D. Khoe, and H. J. S. Dorren, Appl. Phys. B **82**, 615 (2006).
[26]F. Kefelian, S. O'Donoghue, M. T. Todaro, J. G. McInerney, and G. Huyet, IEEE Photonics Technol. Lett. **20**, 1405 (2008).